Alexandria Engineering Journal (2015) 54, 55–64

HOSTED BY
ELSEVIER

Alexandria University

Alexandria Engineering Journal

www.elsevier.com/locate/aej
www.sciencedirect.com

ORIGINAL ARTICLE

Natural convective magneto-nanofluid flow and radiative heat transfer past a moving vertical plate

S. Das [a,*], R.N. Jana [b]

[a] Department of Mathematics, University of Gour Banga, Malda 732 103, India
[b] Department of Applied Mathematics, Vidyasagar University, Midnapore 721 1102, India

Received 29 October 2014; revised 8 December 2014; accepted 12 January 2015
Available online 7 February 2015

KEYWORDS

Natural convection;
Magneto-nanofluid;
Thermal radiation and vertical plate

Abstract An investigation of the hydromagnetic boundary layer flow past a moving vertical plate in nanofluids in the presence of a uniform transverse magnetic field and thermal radiation has been carried out. Three different types of water-based nanofluids containing copper, aluminum oxide and titanium dioxide are taken into consideration. The governing equations are solved using Laplace transform technique and the solutions are presented in closed form. The numerical values of nanofluid temperature, velocity, the rate of heat transfer and the shear stress at the plate are presented graphically for several values of the pertinent parameters. The present study finds applications in engineering devices.

1. Introduction

Nanotechnology has been widely used in many industrial applications. A nanofluid is a term first introduced by Choi [1] and refers to a base liquid with suspended solid nanoparticles. The traditional fluids such as water, mineral oils, and ethylene glycol have a low thermal conductivity where nanofluids have relatively higher thermal conductivity. In the experimental work, Eastman et al. [2] established that an increase in thermal conductivity of approximately 60% can be obtained for a nanofluid consisting of water and 5% vol. of CuO nanoparticles. This is attributed to the increase in surface area due to the suspension of nanoparticles. Also, it was reported that a small amount (less than 1% volume fraction) of copper nanoparticles or carbon nanotubes dispersed in ethylene glycol or oil can increase their inherently poor thermal conductivity by 40% and 50%, respectively [3,4]. For example, copper (Cu) has a thermal conductivity 700 times greater than water and 3000 times greater than engine oil. Das et al. [5] reported a two-to fourfold increase in thermal conductivity enhancement for water-based nanofluids containing Al_2O_3 or CuO nanoparticles over a small temperature range, 21°–51 °C. Keblinski et al. [6] reported on the possible mechanisms of enhancing thermal conductivity. The study of flow characteristics of viscous, incompressible fluids with suspended nano-sized solid particles is highly significant due to application of such fluids in heat

* Corresponding author. Tel.: +91 3222 261171.
E-mail addresses: jana261171@yahoo.co.in, tutusanasd@yahoo.co.in (S. Das).

Peer review under responsibility of Faculty of Engineering, Alexandria University.

http://dx.doi.org/10.1016/j.aej.2015.01.001
1110-0168

transfer devices. Due to the higher thermal conductivity and convective heat transfer rates, nanofluids are used in a wide variety of engineering applications, such as in advanced nuclear systems [7]. The suspension of nanoparticles enhances the thermal conductivity and the convective heat transfer coefficients of several fluids such as oil, water and ethylene glycol mixture. It was shown by Masuda et al. [8] that a characteristic feature of the nanoparticle is to increase the thermal conductivity of the fluid. The topic of heat transfer in nanofluids has been surveyed in review articles by Das and Choi [9], Kakac and Pramuanjaroenkij [10], Wang and Mazumdar [11], Sheikholeslami et al. [12–18], Sheikholeslami and Ganji [19], Sheikholeslami [20], Kandelousi [21], Sheikholeslami and Ganji [22], Sheikholeslami and Ganji [23], Sheikholeslami and Ganji [24], Sheikholeslami and Gorji-Bandpya [25], Sheikholeslami and Ganji [26] and in a book by Das et al. [27].

The study of magnetohydrodynamic (MHD) flow has essential applications in physics, chemistry and engineering. Industrial equipments, such as magnetohydrodynamic (MHD) generators, pumps, bearings and boundary layer control are affected by the interaction between the electrically conducting fluid and a magnetic field. One of the basic and important problems in this area is the hydromagnetic behavior of boundary layers along fixed or moving surfaces in the presence of a transverse magnetic field. MHD boundary layers are observed in various technical systems employing liquid metal and plasma flow transverse of magnetic fields. Recently, many researchers have studied the influences of electrically conducting nanofluids, such as water mixed with a little acid and other ingredients in the presence of a magnetic field on the flow and heat transfer of an incompressible viscous fluid past a moving surface or a stretching plate in a quiescent fluid. Keeping in view, Kuznetsov and Nield [28] have studied the natural convective boundary layer flow of a nanofluid past a vertical plate. Hamad and Pop [29] have investigated the unsteady MHD free convection flow of a nanofluid past a vertical permeable flat plate in a rotating frame of reference with constant heat source. The effects of magnetic field on free convection flow of a nanofluid past a vertical semi-infinite flat plate were studied by Hamad et al. [30]. MHD free convection flow of a nanofluid past a vertical plate in the presence of heat generation or absorption effects has been presented Chamkha and Aly [31]. Turkyilmazoglu [32] has obtained an analytical solution for heat and mass transfer of MHD slip flow in nanofluids. Nandkeolyar et al. [33] have presented the unsteady hydromagnetic radiative flow of a nanofluid past a flat plate with ramped temperature. Turkyilmazoglu and Pop [34] have analyzed the heat and mass transfer of unsteady natural convective flow of nanofluids past a vertical infinite flat plate with radiation effect. The unsteady convective flow of nanofluids past a moving vertical flat plate with heat transfer has been investigated by Turkyilmazoglu [35]. Das [36] has analyzed the flow and heat transfer characteristics of nanofluids in a rotating frame of reference. Sheikholeslami et al. [37] have examined the effect of thermal radiation on a magnetohydrodynamics nanofluid flow and heat transfer by means of two phase model. Sheikholeslami et al. [38] have studied an MHD CuO–water nanofluid flow and convective heat transfer considering Lorentz forces. Sheikholeslami and Ganji [39] have investigated the nanofluid flow past a permeable sheet in a rotating system. Sheikholeslami et al. [40] have described the Lattice Boltzmann method for MHD natural convection heat transfer using nanofluid. The unsteady nanofluid flow and heat transfer in the presence of magnetic field considering thermal radiation have been studied by Sheikholeslami and Ganji [41].

The aim of our present paper was to study the hydromagnetic free convective boundary layer flow of water based nanofluids past a moving vertical infinite flat plate in the presence of a uniform transverse magnetic field and thermal radiation. The fluid flow is assumed to be induced due to the impulsive motion of the plate. Three types of water based nanofluids containing nanoparticles of copper (Cu), aluminum oxide (Al_2O_3) and titanium dioxide (TiO_2) have been considered in the present work. The governing equations are solved analytically and presented in closed form.

2. Formulation of the problem and its solutions

Consider the unsteady free convective flow and heat transfer of a nanofluid past an infinite vertical flat plate moving with an impulsive motion. At time $t = 0$, the plate is at rest with the constant ambient temperature T_∞. At time $t > 0$, the plate starts to move in its own plane with the velocity λu_0 in the vertical direction, where u_0 is constant and the temperature of the plate is raised or lowered to T_w. We choose the x-axis along the plate in the vertical direction and y-axis perpendicular to the plate. A uniform transverse magnetic field of strength B_0 is applied parallel to the y-axis. The plate coincides with the plane $y = 0$ and the flow being confined to $y > 0$. It is assumed that the pressure gradient is neglected in this problem. It is also assumed that a radiative heat flux q_r is applied in the normal direction to the plate. The fluid is a water based nanofluid containing three types nanoparticles Cu, Al_2O_3 and TiO_2. It is further assumed that the base fluid and the suspended nanoparticles are in thermal equilibrium. The thermophysical properties of the nanofluids are given in Table 1. The density is assumed to be linearly dependent on temperature buoyancy forces in the equations of motion. This approximation is exact enough for both dropping liquid and gases at small values of the temperature difference. As the plate is infinitely long, the velocity and temperature fields are functions of y and t only (see Fig. 1).

It is assumed that induced magnetic field produced by the fluid motion is negligible in comparison with the applied one so that we consider magnetic field $\vec{B} \equiv (0, 0, B_0)$. This assumption is justified, since the magnetic Reynolds number is very small for metallic liquids and partially ionized fluids [42]. Also, no external electric field is applied such that the effect of polarization of fluid is negligible [42], so we assume $\vec{E} \equiv (0, 0, 0)$. Under the above assumptions, the momentum and energy equations in the presence of magnetic field and thermal radiation past a moving vertical plate can be expressed as

$$\rho_{nf}\frac{\partial u}{\partial t} = \mu_{nf}\frac{\partial^2 u}{\partial y^2} + g(\rho\beta)_{nf}(T - T_\infty) - \sigma_{nf}B_0^2 u, \tag{1}$$

$$(\rho c_p)_{nf}\frac{\partial T}{\partial t} = k_{nf}\frac{\partial^2 T}{\partial y^2} - \frac{\partial q_r}{\partial y}, \tag{2}$$

where u is the velocity components along the x-direction, T the temperature of the nanofluid, μ_{nf} the dynamic viscosity of the nanofluid, β_{nf} the thermal expansion coefficient of the nanofluid, ρ_{nf} the density of the nanofluid, σ_{nf} the electrical conductivity of the nanofluid, k_{nf} the thermal conductivity of the nanofluid, g the acceleration due to gravity, q_r the radiative

Table 1 Thermo physical properties of water and nanoparticles [43].

Physical properties	Water/base fluid	Cu (copper)	Al_2O_3 (alumina)	TiO_2 (titanium oxide)
ρ (kg/m^3)	997.1	8933	3970	4250
c_p (J/kg K)	4179	385	765	686.2
k (W/m K)	0.613	401	40	8.9538
$\beta \times 10^5$ (K^{-1})	21	1.67	0.85	0.90
ϕ	0.0	0.05	0.15	0.2
σ (S/m)	5.5×10^{-6}	59.6×10^6	35×10^6	2.6×10^6

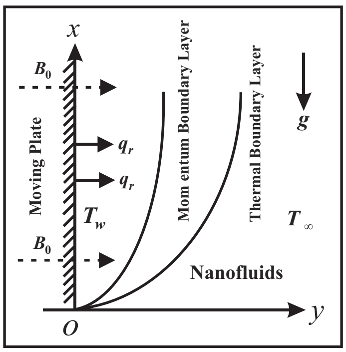

Figure 1 Geometry of the problem.

heat flux and $(\rho c_p)_{nf}$ the heat capacitance of the nanofluid which are given by

$$\begin{aligned}
&\mu_{nf} = \frac{\mu_f}{(1-\phi)^{2.5}}, \quad \rho_{nf} = (1-\phi)\rho_f + \phi\rho_s,\\
&(\rho c_p)_{nf} = (1-\phi)(\rho c_p)_f + \phi(\rho c_p)_s,\\
&(\rho\beta)_{nf} = (1-\phi)(\rho\beta)_f + \phi(\rho\beta)_s,\\
&\sigma_{nf} = \sigma_f\left[1 + \frac{3(\sigma-1)\phi}{(\sigma+2)-(\sigma-1)\phi}\right], \quad \sigma = \frac{\sigma_s}{\sigma_f},
\end{aligned} \tag{3}$$

where ϕ is the solid volume fraction of the nanoparticle, ρ_f the density of the base fluid, ρ_s the density of the nanoparticle, σ_f the electrical conductivity of the base fluid, σ_s the electrical conductivity of the nanoparticle, μ_f the viscosity of the base fluid, $(\rho c_p)_f$ the heat capacitance of the base fluid and $(\rho c_p)_s$ the heat capacitance of the nanoparticle. It is worth mentioning that the expressions (1) are restricted to spherical nanoparticles, where it does not account for other shapes of nanoparticles. The effective thermal conductivity of the nanofluid given by Hamilton and Crosser model followed by Kakac and Pramuanjaroenkij [10], and Oztop and Abu-Nada [43] is given by

$$k_{nf} = k_f\left[\frac{k_s + 2k_f - 2\phi(k_f - k_s)}{k_s + 2k_f + \phi(k_f - k_s)}\right], \tag{4}$$

where k_f is the thermal conductivity of the base fluid and k_s the thermal conductivity of the nanoparticle. In Eqs. (1)–(4), the subscripts nf, f and s denote the thermophysical properties of the nanofluid, base fluid and nanoparticles, respectively.

The initial and boundary conditions are

$$\begin{aligned}
&t = 0 : u = 0, \quad T = T_\infty \quad \text{for all} \quad y \geqslant 0,\\
&t > 0 : u = \lambda u_0, \quad T = T_w \quad \text{at} \quad y = 0,\\
&t > 0 : u \to 0, \quad T \to T_\infty \quad \text{as} \quad y \to \infty,
\end{aligned} \tag{5}$$

where λ denotes the direction of motion of the plate with $\lambda = 0$ for the stationary plate, while $\lambda = \pm 1$ for the forth and back motion of the plate.

It is assumed that the fluid is an optically thick (photon mean free path is very small) gray gas (which emits and absorbs but does not scatter thermal radiation). In an optically thick medium the radiation penetration length is small compare to the characteristic length. The photon mean path is the average distance travelled by a moving photon between successive collisions which modify its direction or energy or other particle properties. For an optically thick fluid, we can adopt Rosseland approximation for radiative flux. The Rosseland approximation [44] applies to optically thick media and gives the net radiation heat flux q_r by the expression

$$q_r = -\frac{4\sigma^*}{3k^*}\frac{\partial T^4}{\partial y}, \tag{6}$$

where $\sigma^*(= 5.67 \times 10^{-8}\ \text{W/m}^2\ \text{K}^4)$ is the Stefan–Boltzmann constant and k^* (m^{-1}) the Rosseland mean absorption coefficient. We assume that the temperature difference within the flow is sufficiently small such that the term T^4 may be expressed as a linear function of temperature. This is done by expanding T^4 in a Taylor series about a free stream temperature T_∞ as follows:

$$T^4 = T_\infty^4 + 3T_\infty^3(T - T_\infty) + 6T_\infty^2(T - T_\infty)^2 + \cdots \tag{7}$$

Neglecting higher-order terms in Eq. (7) beyond the first order in $(T - T_\infty)$, we get

$$T^4 \approx 4T_\infty^3 T - 3T_\infty^4. \tag{8}$$

On the use of Eqs. (6) and (8), Eq. (3) becomes

$$\frac{\partial T}{\partial t} = \frac{1}{(\rho c_p)_{nf}}\left(k_{nf} + \frac{16\sigma^* T_\infty^3}{3k^*}\right)\frac{\partial^2 T}{\partial y^2}, \tag{9}$$

Introducing non-dimensional variables

$$\eta = \frac{u_0 y}{\nu_f}, \quad \tau = \frac{u_0^2 t}{\nu_f}, \quad u_1 = \frac{u}{u_0}, \quad \theta = \frac{T - T_\infty}{T_w - T_\infty}, \tag{10}$$

Eqs. (2) and (9) become

$$\frac{\partial u_1}{\partial \tau} = a_1\frac{\partial^2 u_1}{\partial \eta^2} + \mathrm{Gr}\, a_2\,\theta - M^2 a_3 u_1, \tag{11}$$

$$\frac{\partial \theta}{\partial \tau} = a_4\frac{\partial^2 \theta}{\partial \eta^2}, \tag{12}$$

where

$$x_1 = \left[(1-\phi) + \phi\left(\frac{\rho_s}{\rho_f}\right)\right],$$
$$x_2 = \left[(1-\phi) + \phi\frac{(\rho\beta)_s}{(\rho\beta)_f}\right],$$
$$x_3 = \left[(1-\phi) + \phi\frac{(\rho c_p)_s}{(\rho c_p)_f}\right],$$
$$x_4 = \left[\frac{k_s + 2k_f - 2\phi(k_f - k_s)}{k_s + 2k_f + \phi(k_f - k_s)}\right],$$
$$x_5 = \left[1 + \frac{3(\sigma-1)\phi}{(\sigma+2) - (\sigma-1)\phi}\right], \quad x_6 = \frac{x_4}{x_3},$$
$$a_1 = \frac{1}{(1-\phi)^{2.5}x_1}, \quad a_2 = \frac{x_2}{x_1}, \quad a_3 = \frac{x_5}{x_1}, \quad a_4 = \frac{1}{x_3\mathrm{Pr}}(x_4 + \mathrm{Nr}) \tag{13}$$

and $M^2 = \frac{\sigma_f B_0^2 \nu_f}{\rho_f u_0^2}$ is magnetic parameter, $\mathrm{Nr} = \frac{16\sigma^* T_\infty^3}{3k_f k^*}$ the radiation parameter, $\mathrm{Pr} = \frac{\mu_f c_p}{k_f}$ the Prandtl number and $\mathrm{Gr} = \frac{g\beta_f \nu_f (T_w - T_\infty)}{u_0^3}$ the Grashof number. The magnetic parameter (M^2) is ratio of electromagnetic (Lorentz) force to the viscous force. Grashof number (Gr) that approximates the ratio of the buoyancy force to the viscous force acting. Prandtl number (Pr) is defined as the ratio of momentum diffusivity (kinematic viscosity) to thermal diffusivity. Large Nr signifies a large radiation effect while Nr $\to 0$ corresponds to zero radiation effect.

The corresponding initial and boundary conditions are

$$\begin{aligned} &\tau = 0: u_1 = 0, \quad \theta = 0 \quad \text{for all} \quad \eta \geqslant 0,\\ &\tau > 0: u_1 = \lambda, \quad \theta = 1 \quad \text{at} \quad \eta = 0,\\ &\tau > 0: u_1 \to 0, \quad \theta \to 0 \quad \text{as} \quad \eta \to \infty. \end{aligned} \tag{14}$$

On the use of Laplace transformation, Eqs. (11) and (12) become

$$s\bar{u}_1 = a_1\frac{\partial^2 \bar{u}_1}{\partial \eta^2} + \mathrm{Gr}a_2\bar{\theta} - M^2 a_3 \bar{u}_1, \tag{15}$$

$$s\bar{\theta} = a_4\frac{\partial^2\bar{\theta}}{\partial\eta^2}, \tag{16}$$

where

$$\bar{u}_1(\eta, s) = \int_0^\infty u_1(\eta,\tau)e^{-s\tau}\,d\tau, \quad \bar{\theta}(\eta, s) = \int_0^\infty \theta(\eta,\tau)e^{-s\tau}\,d\tau. \tag{17}$$

The corresponding boundary conditions for $\bar{u}_1$ and $\bar{\theta}$ are

$$\begin{aligned} &\bar{u}_1 = \frac{\lambda}{s}, \quad \bar{\theta} = \frac{1}{s} \quad \text{at} \quad \eta = 0,\\ &\bar{u}_1 \to 0, \quad \bar{\theta} \to 0 \quad \text{as} \quad \eta \to \infty. \end{aligned} \tag{18}$$

Solutions of Eqs. (15) and (15) subject to the boundary conditions (18) are easily obtained and are given by

$$\bar{\phi}(\eta, s) = \frac{1}{s}e^{-\sqrt{\alpha s}\eta}, \tag{19}$$
$$\bar{u}_1(\eta, s) = \frac{\lambda}{s}e^{-\sqrt{s+\gamma}\eta} + \frac{\mathrm{Gr}a_5}{b}\left(\frac{1}{s-b} - \frac{1}{s}\right)\left[e^{-\sqrt{s+\gamma}\eta} - e^{-\sqrt{\alpha s}\eta}\right], \tag{20}$$

where

$$\alpha = \frac{1}{a_4}, \quad \gamma = a_3 M^2, \quad a_5 = \frac{a_2 a_4}{a_1 - a_4}, \quad b = \frac{a_3 a_4 M^2}{a_1 - a_4}. \tag{21}$$

The inverse Laplace transforms of Eqs. (19) and (20) give the solution for the temperature and velocity field as

$$\theta(\eta, \tau) = f_1(\eta\sqrt{\alpha}, \tau), \tag{22}$$
$$u_1(\eta,\tau) = \lambda f_2(\eta,\gamma,\tau) + \frac{\mathrm{Gr}a_5}{b}\left[f_4(\eta,\gamma,b,\tau) - f_3(\eta\sqrt{\alpha}, b, \tau) - f_2(\eta,\gamma,\tau) + f_1(\eta\sqrt{\alpha},\tau)\right], \tag{23}$$

where

$$\begin{aligned} f_1(\eta\sqrt{\alpha},\tau) &= \mathrm{erfc}\left(\frac{\eta\sqrt{\alpha}}{2\sqrt{\tau}}\right),\\ f_2(\eta,\gamma,\tau) &= \frac{1}{2}\left[e^{\eta\sqrt{\gamma}}\mathrm{erfc}\left(\frac{\eta}{2\sqrt{\tau}} + \sqrt{\gamma\tau}\right) + e^{-\eta\sqrt{\gamma}}\mathrm{erfc}\left(\frac{\eta}{2\sqrt{\tau}} - \sqrt{\gamma\tau}\right)\right],\\ f_3(\eta\sqrt{\alpha},\gamma,\tau) &= \frac{1}{2}e^{b\tau}\left[e^{\eta\sqrt{\alpha b}}\mathrm{erfc}\left(\frac{\eta\sqrt{\alpha}}{2\sqrt{\tau}} + \sqrt{b\tau}\right) + e^{-\eta\sqrt{\alpha b}}\mathrm{erfc}\left(\frac{\eta\sqrt{\alpha}}{2\sqrt{\tau}} - \sqrt{b\tau}\right)\right],\\ f_4(\eta,\gamma,b,\tau) &= \frac{1}{2}e^{b\tau}\left[e^{\eta\sqrt{\gamma+b}}\mathrm{erfc}\left(\frac{\eta}{2\sqrt{\tau}} + \sqrt{(\gamma+b)\tau}\right)\right.\\ &\quad\left. + e^{-\eta\sqrt{\gamma+b}}\mathrm{erfc}\left(\frac{\eta}{2\sqrt{\tau}} - \sqrt{(\gamma+b)\tau}\right)\right], \end{aligned} \tag{24}$$

where α, b, a_5 and γ are given by (21) and erfc(.) being the complementary error function.

3. Results and discussion

In order to get a clear insight on the physics of the problem, a parametric study is performed and the obtained numerical results are elucidated with the help of graphical illustrations. We have presented the non-dimensional fluid velocity u_1 and the fluid temperature θ for several values of magnetic parameter M^2, Grashof number Gr, radiation parameter Nr, volume fraction parameter ϕ and time τ in Figs. 2–10. The values of volume fraction of nanoparticles are taken in the range of $0 \leqslant \phi \leqslant 0.2$. The case $M^2 = 0$ corresponds to the absence of magnetic field and $\phi = 0$ for regular fluid. The default values of the other parameters are mentioned in the description of the respected figures.

3.1. Effects of parameters on velocity profiles

The non-dimensional velocity distribution for three types of nanoparticles (Cu, Al_2O_3 and TiO_2) and constant solid volume

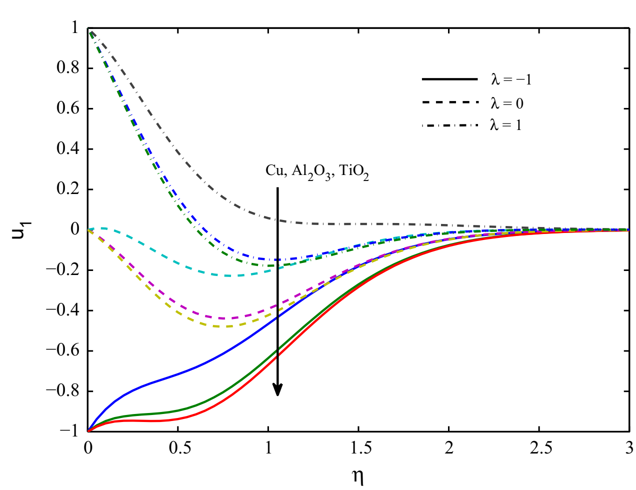

Figure 2 Velocity profile for different nanofluids when $M^2 = 5$, $\phi = 0.1, \mathrm{Gr} = 5, \mathrm{Nr} = 0.5$ and $\tau = 0.5$.

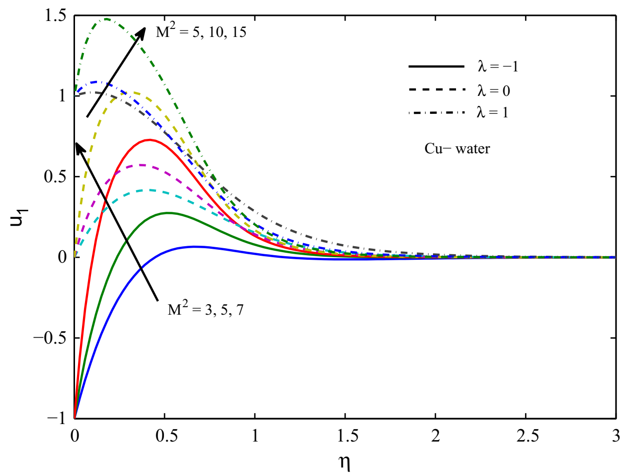

Figure 3 Velocity u_1 for different M^2 when $\mathrm{Gr} = 5$, $\mathrm{Nr} = 0.5$, $\phi = 0.1$ and $\tau = 0.5$.

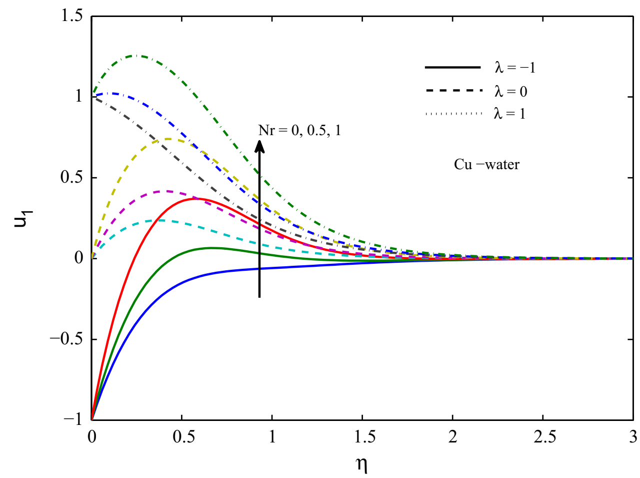

Figure 6 Velocity u_1 for different Nr when $M^2 = 5$, $\phi = 0.1$, $\mathrm{Gr} = 5$ and $\tau = 0.5$.

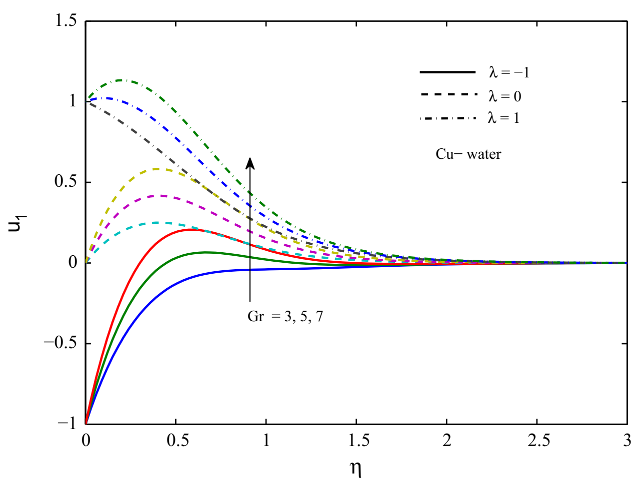

Figure 4 Velocity u_1 for different Gr when $M^2 = 5$, $\mathrm{Nr} = 0.5$, $\phi = 0.1$ and $\tau = 0.5$.

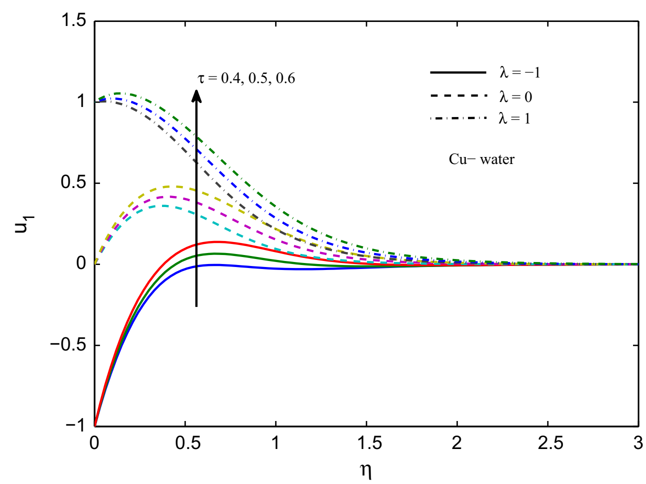

Figure 7 Velocity u_1 for different time τ when $M^2 = 5$, $\mathrm{Nr} = 0.5$, $\mathrm{Gr} = 5$ and $\phi = 0.1$.

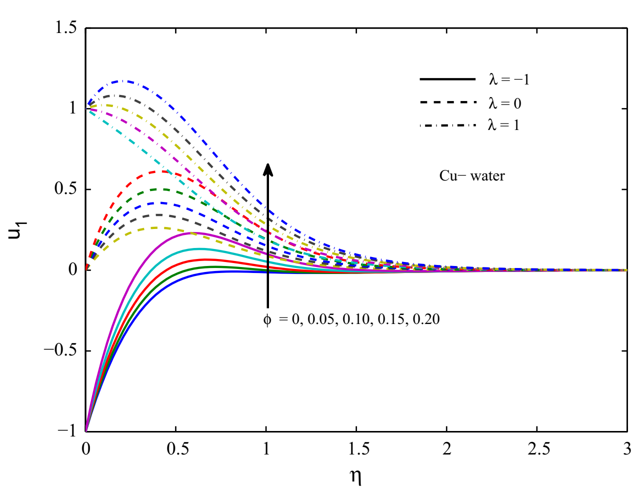

Figure 5 Velocity u_1 for different ϕ when $M^2 = 5$, $\mathrm{Nr} = 0.5$, $\mathrm{Gr} = 5$ and $\tau = 0.5$.

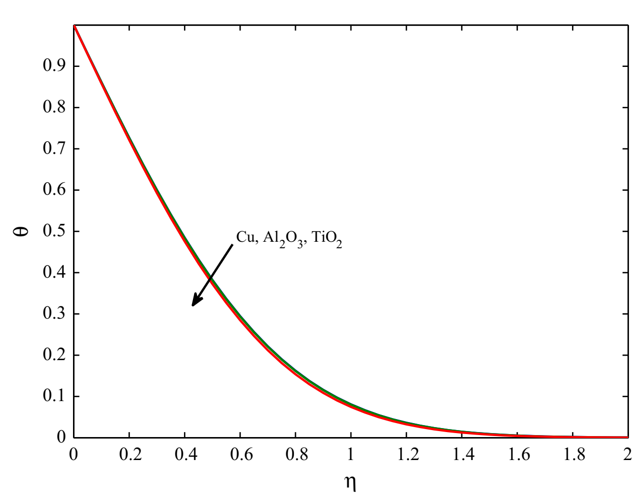

Figure 8 Temperature for different nanofluids when $\mathrm{Nr} = 0.5$, $\phi = 0.1$, $\mathrm{Pr} = 6.2$ and $\tau = 0.5$.

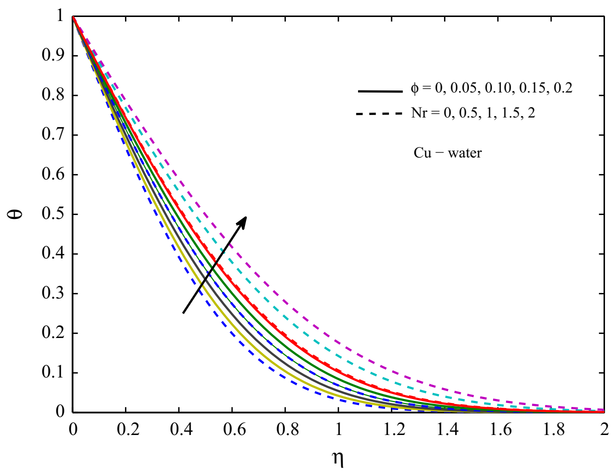

Figure 9 Temperature for different ϕ and Nr when $\tau = 0.5$ and $\mathrm{Pr} = 6.2$.

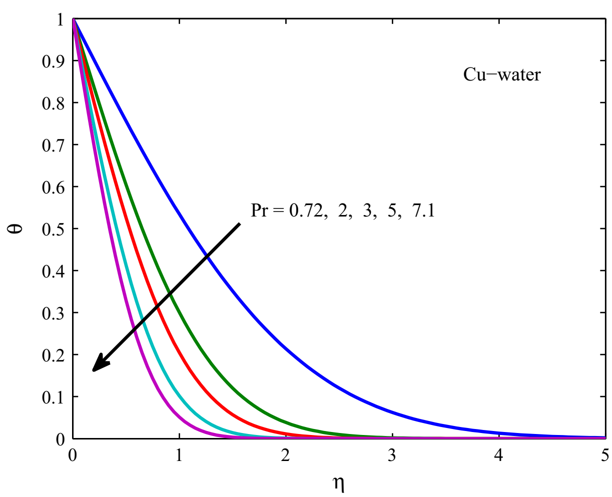

Figure 10 Temperature for different Pr when $\mathrm{Nr} = 0.5, \tau = 0.5$ and $\phi = 0.1$.

fraction is shown in Fig. 2. It is obvious that the velocity distributions for Al_2O_3–water and TiO_2–water are almost the same as their densities are near to each other, but due to high density of Cu, for Cu–water the dynamic viscosity increases more and leads to a thinner boundary layer than other particles for the cases of stationary plate ($\lambda = 0$) as well as moving plate ($\lambda = \pm 1$). Fig. 3 reveals that the fluid velocity u_1 accelerates for increasing values of magnetic parameter M^2. The momentum boundary layer thickness increases for increasing values of M^2 for the cases of stationary plate ($\lambda = 0$) as well as moving plate ($\lambda = \pm 1$). The velocity profiles are characterized by distinctive peaks in the immediate vicinity of the plate and as M^2 increases these peaks decrease and move gradually downstream. This is due to the fact that the magnetic lines of forces move past the plate and the fluid which is decelerated by the viscous force, receives a push from the magnetic field which counteracts the viscous effects. Hence the velocity of the fluid increases as the parameter M^2 increases. Fig. 4 shows that the velocity u_1 increases with an increase in Grashof number Gr for the cases of stationary plate ($\lambda = 0$) as well as moving plate ($\lambda = \pm 1$). This trend is due to the fact that the positive Grashof number Gr acts like a favorable pressure gradient which accelerates the fluid in the boundary layer. Consequently, the velocity increases with Gr. Grashof number represents the effect of free convection currents. Physically, $\mathrm{Gr} > 0$ means heating of the fluid of cooling of the boundary surface, $\mathrm{Gr} < 0$ means cooling of the fluid of heating of the boundary surface and $\mathrm{Gr} = 0$ corresponds the absence of free convection current.

Fig. 5 depicts the effect of solid volume fraction ϕ of nanoparticles on the fluid velocity. The fluid velocity u_1 increases for increasing values of ϕ for the cases of stationary plate ($\lambda = 0$) as well as moving plate ($\lambda = \pm 1$). It is also revealed that the increase in the values of ϕ results in the increase of the momentum boundary layer thickness. The effect of radiation parameter Nr on the velocity profiles is presented in Fig. 6. The fluid velocity u_1 enhances as the value of Nr increases for both cases of stationary plate ($\lambda = 0$) as well as moving plate ($\lambda = \pm 1$). The velocity profiles increase sharply near the surface of the plate and after attaining respective maxima's, the curves settle down to the corresponding asymptotic value. Therefore, Nr behaves like a supporting force which accelerates the fluid particles near the vicinity of the plate. Also, it is noted that momentum boundary layer thickness increases when Nr tends to increase inside a boundary layer region. Fig. 7 reveals that the fluid velocity u_1 increases as time τ increases for both cases of stationary plate ($\lambda = 0$) as well as moving plate ($\lambda = \pm 1$).

3.2. Effects of parameters on temperature profiles

Fig. 8 reveals the fluid temperature variations for the three types of water-based nanofluids Cu–water, Al_2O_3–water and TiO_2–water. However, due to higher thermal conductivity of Cu–water nanofluids, the temperature of Cu–water nanofluid is found to be higher than Al_2O_3–water and TiO_2–water nanofluids. It is also seen that the thermal boundary layer thickness is more for Cu–water than Al_2O_3–water and TiO_2–water nanofluids. Fig. 9 displays the effect of volume fraction ϕ of nanoparticles and radiation parameter Nr on the temperature distribution. The fluid temperature increases as volume fraction parameter ϕ enlarges. Also, the thermal boundary layer for Cu–water is greater than for pure water ($\phi = 0$). This is because copper has high thermal conductivity and its addition to the water based fluid increases the thermal conductivity for the fluid, so the thickness of the thermal boundary layer increases. It is also observed that with increasing the volume fraction ϕ of the nanoparticles the thermal boundary layer is increased. This agrees with the physical behavior of nanoparticles. This observation shows that the use of nanofluids will be significance in the cooling and heating processes. The increase in radiation parameter means the release of heat energy from the flow region and so the fluid temperature decreases. A decrease in the values of Nr for given k_{nf} and T_∞ means a decrease in the Rosseland radiation absorptivity k^*. Since divergence of the radiative heat flux $\frac{\partial q_r}{\partial y}$ increases, k^* decreases which in turn causes to increase the rate of radiative heat transfer to the fluid and hence the fluid temperature increases. This means that the thermal boundary layer decreases and more uniform temperature distribution across the boundary layer. Fig. 10 represents the variation of nanofluid temperature for Prandtl number Pr. The temperature profiles exhibit that the fluid temperature decreases as Pr increases. This is due to the fact that a higher Prandtl number fluid has relatively low thermal conductivity, which reduces conduction and there by the thermal boundary layer thickness; and as a result, temperature decreases. Fig. 11 reveals that temperature increases with increasing time τ. The fluid temperature is high near the plate and decreases asymptotically to the free stream with zero- value far away from the plate.

3.3. Effects of parameters on rate of heat transfer at the plate

The rate of heat transfer at the plate $\eta = 0$ is given by

$$\theta'(0,\tau) = \left(\frac{\partial\theta}{\partial\eta}\right)_{\eta=0} = -\sqrt{\frac{\alpha}{\pi\tau}}. \tag{25}$$

Numerical results of the rate of heat transfer $\theta'(0,\tau)$ at the plate $\eta = 0$ are presented in the Figs. 12–14 for several values of volume fraction parameter ϕ, radiation parameter Nr and time τ. The rate of heat transfer $\theta'(0)$ is found to variate in case of different nanofluids as shown in Fig. 12. Since the thermal conductivity of Cu is higher than Al_2O_3, the rate of heat transfer is found to be higher for Cu–water nanofluid. Fig. 12 shows that the rate of heat transfer $\theta'(0,\tau)$ enhances for increasing values of radiation parameter Nr. This can be realized from the fact that as thermal radiation increases, the dominance effect of temperature gradient increases, leading to an increase in the rate of heat transfer. Fig. 13 illustrates that the rate of heat transfer $\theta'(0,\tau)$ increases as ϕ enlarges. This is due to increase in thermal conductivity with the solid volume fraction of nanoparticles. Also, the thermal boundary layer thickness decreases with increase of nanoparticle volume fraction and in turn the rate of heat transfer increases with increase of volume fraction of nanoparticles. This fact is also reported by Turkyilmazoglu and Pop [34]. Further, Fig. 13 reveals that the rate of heat transfer $\theta'(0,\tau)$ enhances as time τ progresses. The negative value of $\theta'(0,\tau)$ signifies that the heat flows from fluid to the plate. This is because there is significant heat generation near the moving plate then the temperature of the fluid near the moving plate may exceed the plate temperature. This causes flow of heat from the fluid to the moving plate even if the temperature is higher than the ambient temperature. It is

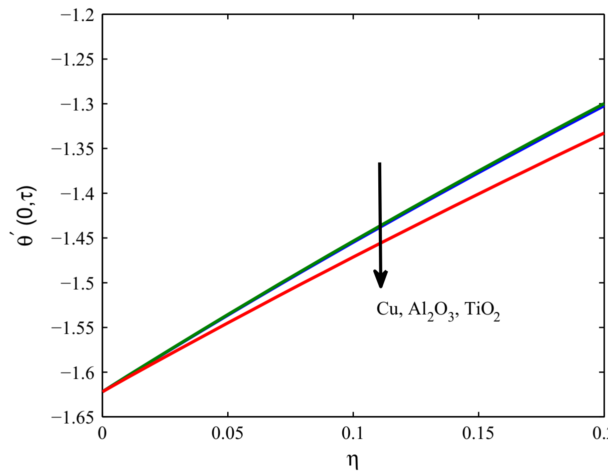

Figure 12 Rate of heat transfer $\theta'(0,\tau)$ for different nanofluids when $Nr = 0.5, Pr = 6.2$ and $\tau = 0.5$.

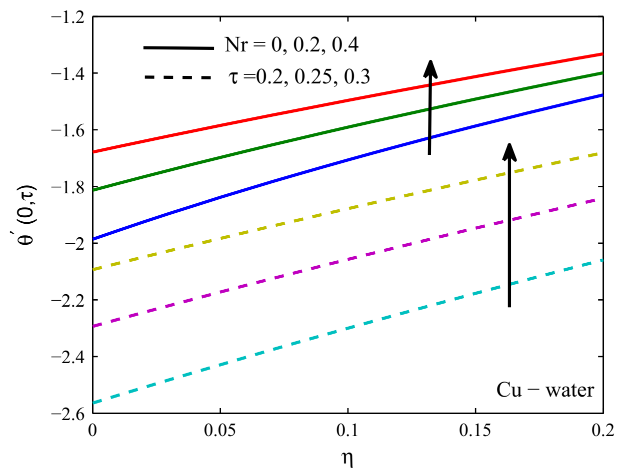

Figure 13 Rate of heat transfer $\theta'(0,\tau)$ for different Nr and time τ when $Pr = 6.2$.

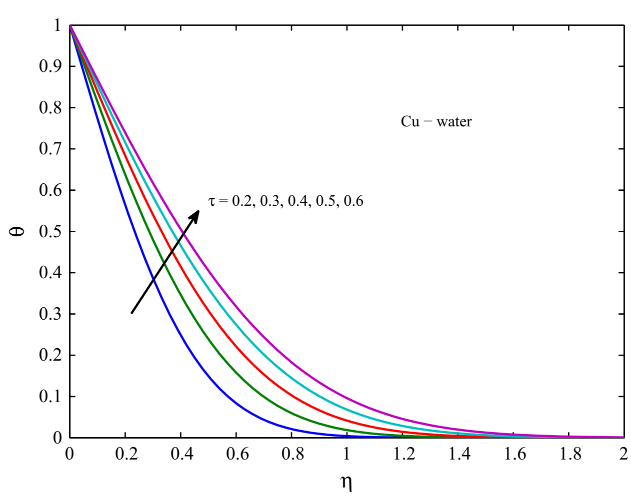

Figure 11 Temperature for different time τ when $Nr = 0.5, Pr = 6.2$ and $\phi = 0.1$.

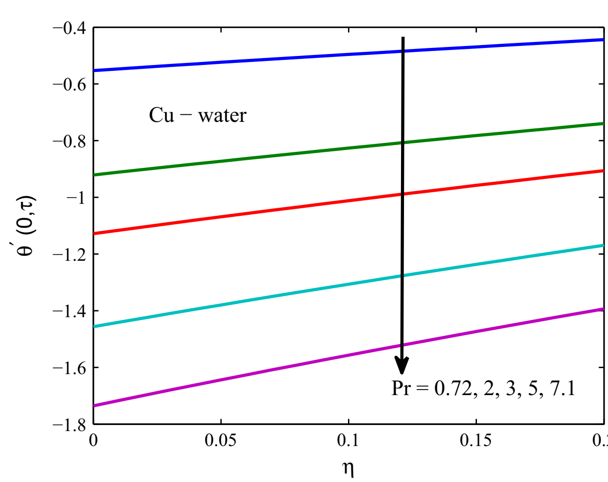

Figure 14 Rate of heat transfer $\theta'(0,\tau)$ for different Pr when $Nr = 0.5$ and $\tau = 0.5$.

seen from the Fig. 14 that the rate of heat transfer $\theta'(0,\tau)$ at the plate reduces for increasing values of Pr. Physically, when fluid attains a higher Prandtl number, its thermal conductivity is decreased and so its heat conduction capacity diminishes. Thereby the thermal boundary layer thickness is reduced. As a consequence, the heat transfer rate at the plate is reduced as Prandtl number increases.

3.4. Effects of parameters on the shear stress at the plate

For the sake of engineering purposes, one is usually interested to evaluate the shear stress (or skin friction). The increased shear stress is generally a disadvantage in the technical applications.The non-dimensional shear stress at the plate $\eta = 0$ due to the flow is given by

$$\tau_x = -\left(\frac{\partial u_1}{\partial \eta}\right)_{\eta=0} = \lambda\left[\sqrt{\gamma}\operatorname{erf}(\sqrt{\gamma\tau}).+\frac{e^{-\gamma\tau}}{\sqrt{\pi\tau}}\right] + \frac{\mathrm{Gr}a_5}{b}\left[e^{b\tau}\left\{\sqrt{\gamma+b}\operatorname{erf}\left(\sqrt{(\gamma+b)\tau}\right) - \sqrt{\alpha b}\ \operatorname{erf}\left(\sqrt{b\tau}\right)\right\} - \sqrt{\gamma}\ \operatorname{erf}(\sqrt{\gamma\tau})\right], \tag{26}$$

where α, b, a_5 and γ are given by (21).

Numerical values of the non-dimensional shear stress τ_x at the plate $\eta = 0$ are presented in Figs. 15–19 for several values of volume fraction parameter ϕ, magnetic parameter M^2, Grashof number Gr, radiation parameter Nr and time τ. The variation of the shear stress τ_x with different nanofluids is shown in Fig. 15. Since the density of Cu–water nanofluid is higher than Al_2O_3 and TiO_2–water nanofluids, the shear stress for Cu–water nanofluid is found to be lower. Figs. 16 shows that the shear stress τ_x at the plate $\eta = 0$ due to the fluid flow decreases with an increase in magnetic parameter M^2. Also, it is seen from Figs. 17–19 that the shear stress τ_x due to the fluid flow decreases with an increase in either Grashof number Gr or radiation parameter Nr or time τ for the cases of stationary plate ($\lambda = 0$) as well as moving plate ($\lambda = \pm 1$). Since the positive buoyancy force acts like a favorable pressure gradient, the fluid in the boundary layer is accelerated. Consequently, the hot fluid near the plate surface is carried away more quickly as Grashof

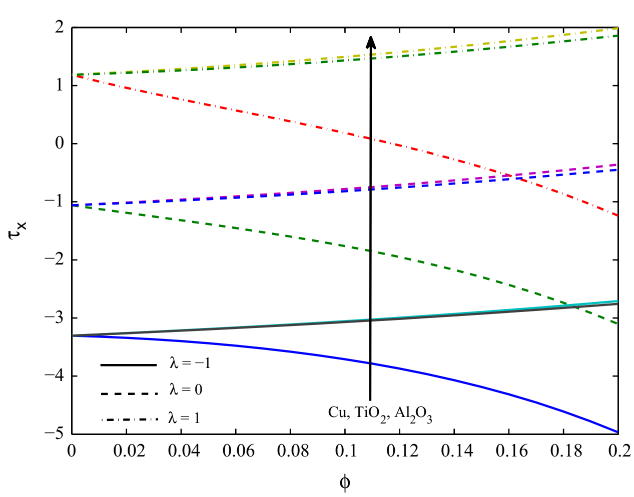

Figure 15 Shear stress τ_x for different nanofluids when $M^2 = 5$, Gr = 5, Nr = 0.5 and $\tau = 0.5$.

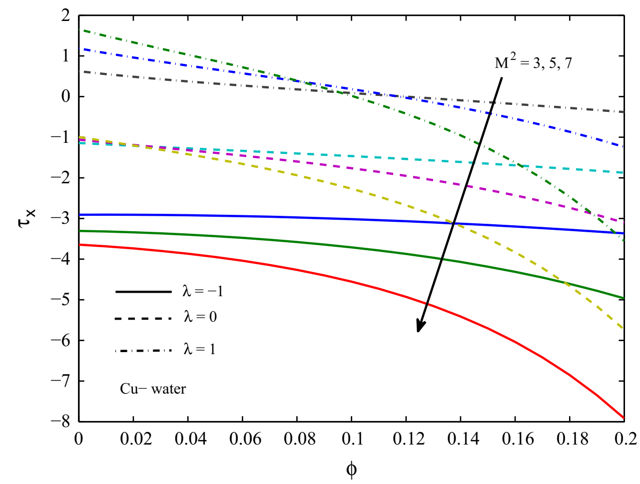

Figure 16 Shear stress τ_x for different M^2 when Gr = 5, Nr = 0.5 and $\tau = 0.5$.

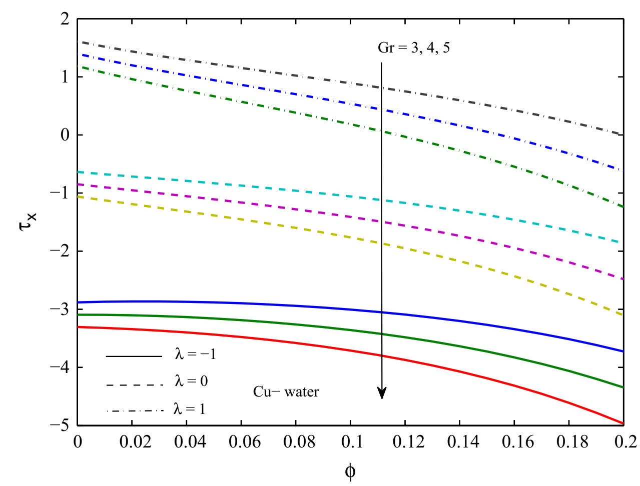

Figure 17 Shear stress τ_x for different Gr when $M^2 = 5$, Nr = 0.5 and $\tau = 0.5$.

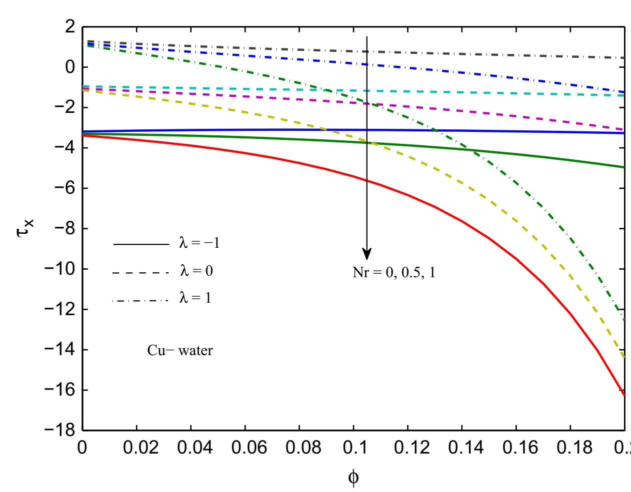

Figure 18 Shear stress τ_x for different Nr when Gr = 5, $M^2 = 5$ and $\tau = 0.5$.

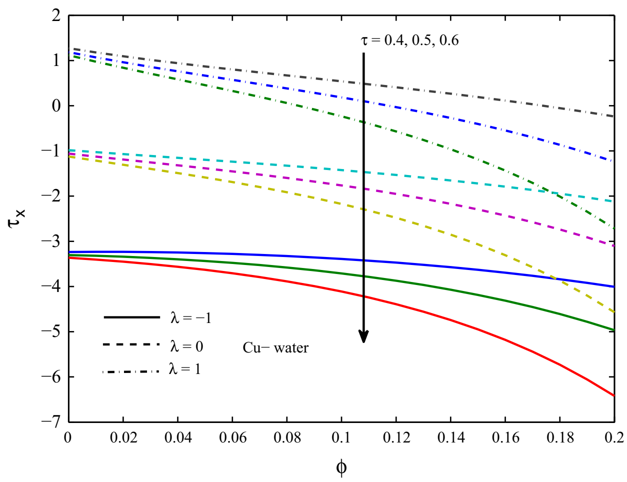

Figure 19 Shear stress τ_x for different time τ when $\mathrm{Gr} = 5$, $\mathrm{Nr} = 0.5$ and $M^2 = 5$.

number Gr increases. Therefore, the shear stress τ_x at the plate reduces. The shear stress τ_x is a decreasing function of volume fraction ϕ of nanoparticle. The negative value of τ_x means that the plate exerts a drag force on the fluid (and vice versa).

4. Conclusion

The purpose of this study is to obtain exact solutions for the unsteady natural convection boundary layer flow of a nanofluid near a moving infinite vertical plate in the presence of a transverse uniform magnetic field. Rosseland diffusion approximation is used to describe the radiative heat flux in the energy equation. The expressions for the velocity and the temperature have been obtained in closed form with the help of the Laplace transform technique. The effects of the pertinent parameters on velocity and temperature profiles are presented graphically. The influences of the same parameters on the shear stress and rate of heat transfer at the plate are also discussed in details. The most important concluding remarks can be summarized as follows:

- An increase in radiation parameter leads to decrease the fluid velocity as well as temperature in the boundary layer region.
- An increase in Grashof number and an increase in time lead to increase the fluid velocity and temperature.
- The rate of heat transfer at the plate is found to be higher for Cu–water nanofluid.
- The shear stress at the plate for Cu–water nanofluid is found to be lower.

References

[1] S.U.S. Choi, Enhancing thermal conductivity of fluids with nanoparticles developments and applications of non-Newtonian flows, ASME FED 231/MD 66 (1995) 99–105.

[2] J.A. Eastman, S.U.S. Choi, S. Li, L.J. Thompson, S. Lee, Enhanced thermal conductivity through the development of nanofluids, in: S. Komarneni, J.C. Parker, H.J. Wollenberger (Eds.), Nanophase and Nanocomposite Materials II, Materials Research Society, Pittsburgh, 1997.

[3] J.A. Eastman, S.U.S. Choi, S. Li, W. Yu, L.J. Thompson, Anomalously increased effective thermal conductivities of ethylene glycol-based nano-fluids containing copper nanoparticles, Appl. Phys. Lett. 78 (2001) 718–720.

[4] S.U.S. Choi, Z.G. Zhang, W. Yu, F.E. Lockwood, E.A. Grulke, Anomalously thermal conductivity enhancement in nanotube suspensions, Appl. Phys. Lett. 79 (2001) 22522254.

[5] S.K. Das, N. Putra, P. Thiesen, W. Roetzel, Temperature dependence of thermal conductivity enhancement for nanofluids, J. Heat Transfer 125 (2003) 567–574.

[6] P. Keblinski, S.R. Phillpot, S.U.S. Choi, J.A. Eastman, Mechanism of heat flow is suspensions of nano-sized particles (nanofluids), Int. J. Heat Mass Tranfer 42 (2002) 855–863.

[7] J. Buongiorno, W. Hu, Nanofluid coolants for advanced nuclear power plants, in: Proceedings of ICAPP05, Seoul, 2005.

[8] H. Masuda, A. Ebata, K. Teramae, N. Hishinuma, Alteration of thermal conductivity and viscosity of liquids by dispersing ultra-fine particles, Netsu Busse. 7 (1993) 227–233.

[9] S.K. Das, S.U. Choi, A review of heat transfer in nanofluids, Adv. Heat Transfer 46 (2009) 119.

[10] S. Kakac, A. Pramuanjaroenkij, Review of convective heat transfer enhancement with nanofluids, Int. J. Heat Mass Transfer 52 (2009) 3187–3196.

[11] X.Q. Wang, A.S. Mazumdar, Heat transfer characteristics of nanofluids: a review, Int. J. Therm. Sci. 46 (2007) 119.

[12] M. Sheikholeslami, D.D. Ganjia, M.M. Rashidib, Ferrofluid flow and heat transfer in a semi annulus enclosure in the presence of magnetic source considering thermal radiation, J. Taiwan Inst. Chem. Eng. (2014), http://dxdoi.org/10.1016/j.jtice.2014.09.026.

[13] M. Sheikholeslami, M. Hatami, G. Domairry, Numerical simulation of two phase unsteady nanofluid flow and heat transfer between parallel plates in presence of time dependent magnetic field, J. Taiwan Inst. Chem. Eng. (2014), http://dxdoi.org/10.1016/j.jtice.2014.09.025.

[14] M. Sheikholeslami, M. Gorji-Bandpya, K. Vajravelu, Lattice Boltzmann simulation of magnetohydrodynamic natural convection heat transfer of Al_2O_3–water nanofluid in a horizontal cylindrical enclosure with an inner triangular cylinder, Int. J. Heat Mass Transfer 80 (2015) 16–25.

[15] M. Sheikholeslami, S. Abelman, D.D. Ganji, Numerical simulation of MHD nanofluid flow and heat transfer considering viscous dissipation, Int. J. Heat Mass Transfer 79 (2014) 212–222.

[16] M. Sheikholeslami, M. Gorji-Bandpya, D.D. Ganji, Investigation of nanofluid flow and heat transfer in presence of magnetic field using KKL model, Arab. J. Sci. Eng. 39 (6) (2014) 5007–5016.

[17] M. Sheikholeslami, M. Gorji-Bandpya, D.D. Ganji, MHD free convection in an eccentric semi-annulus filled with nanofluid, J. Taiwan Inst. Chem. Eng. 45 (2014) 1204–1216.

[18] M. Sheikholeslami, M. Gorji-Bandpya, D.D. Ganji, Numerical investigation of MHD effects on Al_2O_3–water nanofluid flow and heat transfer in a semi-annulus enclosure using LBM, Energy 60 (2013) 501–510.

[19] M. Sheikholeslami, D.D. Ganji, Entropy generation of nanofluid in presence of magnetic field using lattice Boltzmann method, Physica A. http://dx.doi.org/10.1016/j.physa.2014.09.053.

[20] M. Sheikholeslami, Effect of uniform suction on nanofluid flow and heat transfer over a cylinder, J. Braz. Soc. Mech. Sci. Eng. (2014), http://dxdoi.org/10.1007/s40430-014-0242-z.

[21] M.S. Kandelousi, KKL correlation for simulation of nanofluid flow and heat transfer in a permeable channel, Phys. Lett. A. http://dx.doi.org/10.1016/j.physleta.2014.09.046.

[22] M. Sheikholeslami, D.D. Ganji, Ferrohydrodynamic and magnetohydrodynamic effects on ferrofluid flow and convective heat transfer, Energy 75 (2014) 400–410.

[23] M. Sheikholeslami, D.D. Ganji, Heated permeable stretching surface in a porous medium using nanofluids, J. Appl. Fluid Mech. 7 (3) (2014) 535–542.
[24] M. Sheikholeslami, D.D. Ganji, Magnetohydrodynamic flow in a permeable channel filled with nanofluid, Sci. Iran. B 21 (1) (2014) 203–212.
[25] M. Sheikholeslami, M. Gorji-Bandpya, Free convection of ferrofluid in a cavity heated from below in the presence of an external magnetic field, Powder Technol. 256 (2014) 490–498.
[26] M. Sheikholeslami, D.D. Ganji, Three dimensional heat and mass transfer in a rotating system using nanofluid, Powder Technol. 253 (2014) 789–796.
[27] S.K. Das, U.S. Choi, W. Yu, T. Pradeep, Nanofluids: Science and Technology, Wily, 2008.
[28] A.V. Kuznetsov, D.A. Nield, Natural convective boundary-layer flow of a nanofluid past a vertical plate, Int. J. Therm. Sci. 49 (2010) 243–247.
[29] M A A Hamad, I. Pop, Unsteady MHD free convection flow past a vertical permeable flat plate in a rotating frame of reference with constant heat source in a nanofluid, Heat Mass Transfer 47 (2011) 1517–1524.
[30] M.A.A. Hamad, I. Pop I, I.A.M. Ismail, Magnetic field effects on free convection flow of a nanofluid past a vertical semi-infinite flat plate, Nonlinear Anal. Real World Appl. 12 (3) (2011) 1338–1346.
[31] A.J. Chamkha, A.M. Aly, MHD free convection flow of a nanofluid past a vertical plate in the presence of heat generation or absorption effects, Chem. Eng. Commun. 198 (2011) 425–441.
[32] M. Turkyilmazoglu, Exact analytical solutions for heat and mass transfer of MHD slip flow in nanofluids, Chem. Eng. Sci. 84 (2014) 182–187.
[33] R. Nandkeolyar, M. Das, H. Pattnayak, Unsteady hydromagnetic radiative flow of a nanofluid past a flat plate with ramped temperature, J. Orissa Math. Soc. 32 (1) (2013) 15–30.
[34] M. Turkyilmazoglu, I. Pop, Heat and mass transfer of unsteady natural convection flow of some nanofluids past a vertical infinite flat plate with radiation effect, Int. J. Heat Mass Transfer 59 (2013) 167–171.
[35] M. Turkyilmazoglu, Unsteady convection flow of some nanofluids past a moving vertical flat plate with heat transfer, ASME J. Heat Transfer 136 (2014), 031704-1.
[36] K. Das, Flow and heat transfer characteristics of nanofluids in a rotating frame, Alexandria Eng. J. (2014), http://dxdoi.org/10.1016/j.aej.2014.04.003.
[37] M. Sheikholeslami, D.D. Ganji, M.Y. Javedb, R. Ellahi, Effect of thermal radiation on magnetohydrodynamics nanofluid flow and heat transfer by means of two phase model, J. Magn. Magn. Mater. 374 (2015) 36–43.
[38] M. Sheikholeslami, M. Gorji Bandpy, R. Ellahi, A. Zeeshan, Simulation of MHD CuO–water nanofluid flow and convective heat transfer considering Lorentz forces, J. Magn. Magn. Mater. 369 (2014) 69–80.
[39] M. Sheikholeslami, D.D. Ganji, Numerical investigation for two phase modeling of nanofluid in a rotating system with permeable sheet, J. Mol. Liq. 194 (2014) 13–19.
[40] M. Sheikholeslami, M. Gorji-Bandpya, D.D. Ganji, Lattice Boltzmann method for MHD natural convection heat transfer using nanofluid, Powder Technol. 254 (2014) 82–93.
[41] M. Sheikholeslami, D.D. Ganji, Unsteady nanofluid flow and heat transfer in presence of magnetic field considering thermal radiation, J. Braz. Soc. Mech. Sci. Eng.. http://dx.doi.org/10.1007/s40430-014-0228-x.
[42] K.R. Cramer, S.I. Pai, Magnetofluid Dynamics for Engineers and Applied Physicists, McGraw-Hill, New York, 1973.
[43] H.F. Oztop, E. Abu-Nada, Numerical study of natural convection in partially heated rectangular enclosures filled with nanofluids, Int. J. Heat Fluid Flow 29 (2008) 1326–1336.
[44] S. Rosseland, Astrophysik und atom-theoretische Grundlagen, Springer-Verlag, Berlin, 1931.